



Supplementary Materials for

Structures of Respiratory Syncytial Virus G Antigen Bound to Broadly-Neutralizing Antibodies

Stanislav O. Fedechkin, Natasha L. George, Jacob T. Wolff, Lawrence M. Kauvar,
Rebecca M. DuBois*

*correspondence to: rmdubois@ucsc.edu

This PDF file includes:

Fig. S1. Co-elution of RSV G-antibody complexes in solution.

Fig. S2. Electron density maps and structural alignments of RSV G.

Fig. S3. Schematic of RSV G interactions with anti-G antibodies.

Fig. S4. Structural comparison of RSV G with CX3CL1 (fractalkine).

Fig. S5. Isolated human anti-G mAbs and epitope characterization.

Table S1. Crystallographic data collection and refinement statistics.

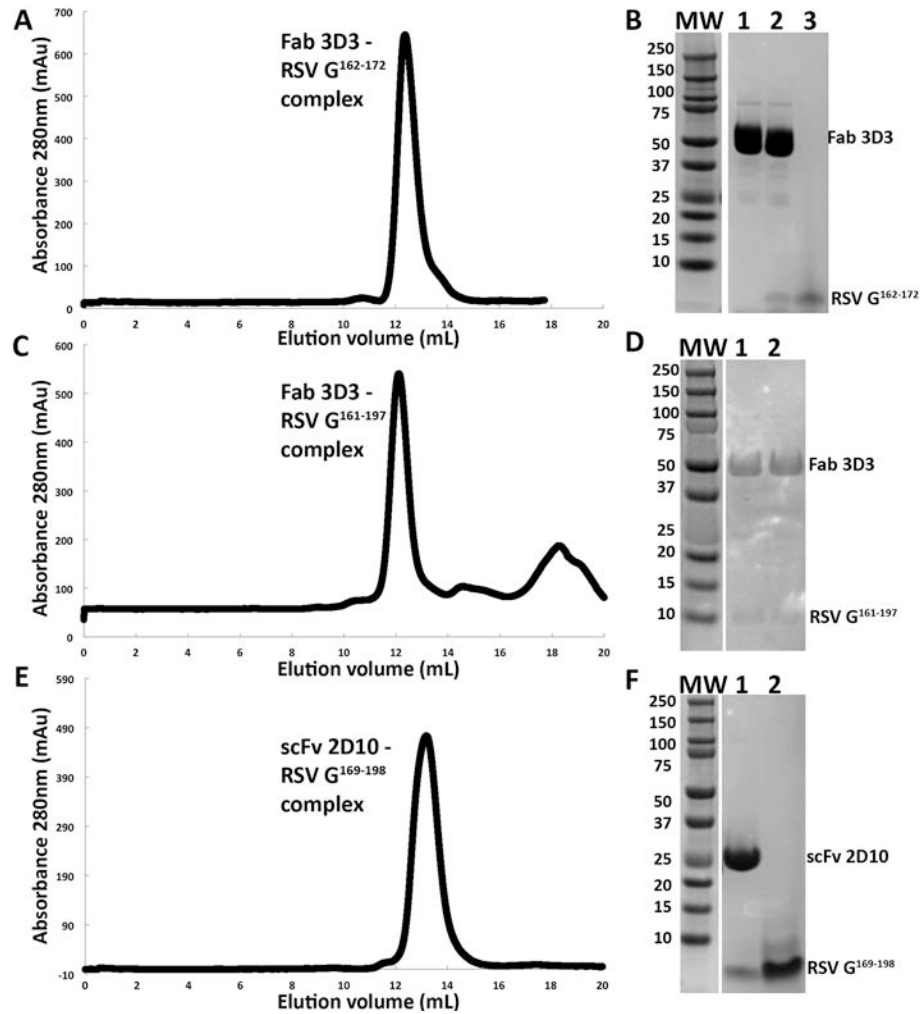


Fig. S1. Co-elution of RSV G-antibody complexes in solution. (A, C, E) Superdex 200 size-exclusion chromatography purification traces of antibody-RSV G complexes. (B) Non-reducing SDS-PAGE of molecular weight markers in kD (MW), Fab 3D3 alone (lane 1), co-eluted Fab 3D3-RSV G¹⁶²⁻¹⁷² complex (lane 2), and RSV G¹⁶²⁻¹⁷² alone (lane 3). (D) Non-reducing SDS-PAGE of molecular weight markers in kD (MW) and co-eluted Fab 3D3-RSV G¹⁶¹⁻¹⁹⁷ complex (lanes 1 and 2). (F) Reducing SDS-PAGE of molecular weight markers in kD (MW), co-eluted scFv 2D10-RSV G¹⁶⁹⁻¹⁹⁸ complex (lane 1), and RSV G¹⁶⁹⁻¹⁹⁸ alone (lane 2).

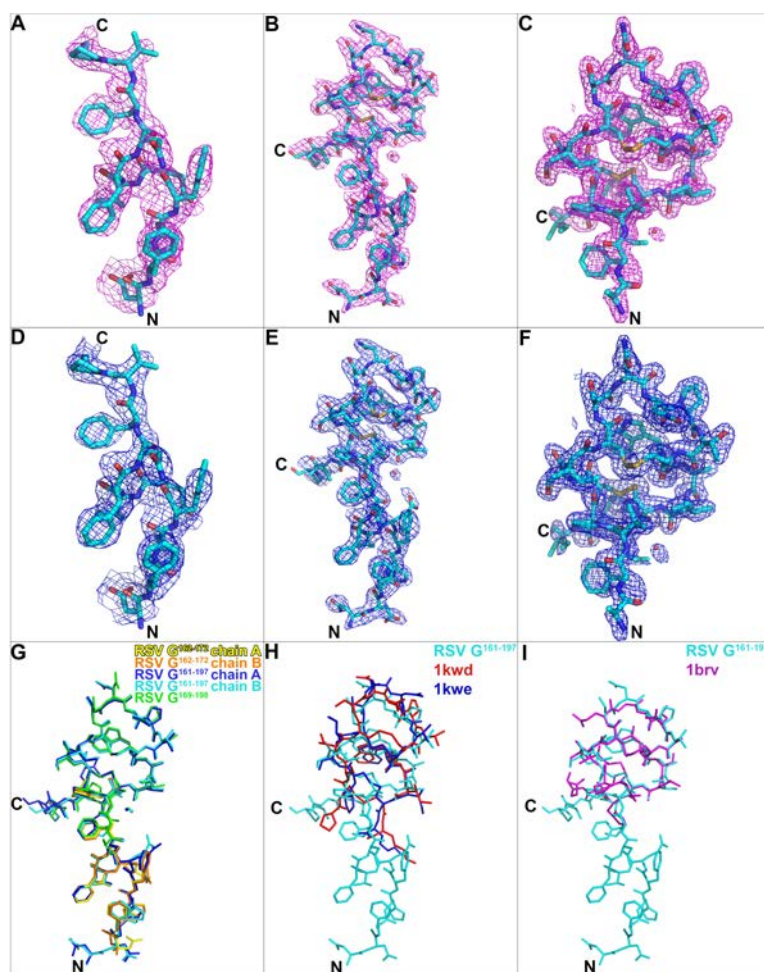


Fig. S2. Electron density maps and structural alignments of RSV G. (A, D) Electron density maps around RSV G¹⁶²⁻¹⁷² (when bound to Fab 3D3), (B, E) Electron density maps around RSV G¹⁶¹⁻¹⁹⁷ (when bound to Fab 3D3). (C, F) Electron density maps around RSV G¹⁶⁹⁻¹⁹⁸ (when bound to scFv 2D10). The 2Fo-Fc electron density maps (in pink, panels A-C) and unbiased composite omit maps (in blue, panels D-F) are contoured at 1.0 σ . (G) Structural alignment of RSV G from all three structures. Note that in the Fab 3D3-RSV G¹⁶²⁻¹⁷² complex and Fab 3D3-RSV G¹⁶¹⁻¹⁹⁷ complex structures, there are two molecules of RSV G in the asymmetric unit. (H) Structural alignment of RSV G¹⁶¹⁻¹⁹⁷ with human RSV G cysteine noose structures determined previously by NMR (PDB entries 1kwd and 1kwe). The RMSD for the alignment of RSV G¹⁶¹⁻¹⁹⁷ with 1kwd is 1.0 Å and with 1kwe is 1.4 Å. (I) Structural alignment of RSV G¹⁶¹⁻¹⁹⁷ with bovine RSV G cysteine noose structure determined previously by NMR (PDB entries 1brv). The RMSD for the alignment of RSV G¹⁶¹⁻¹⁹⁷ with 1brv is 0.7 Å.

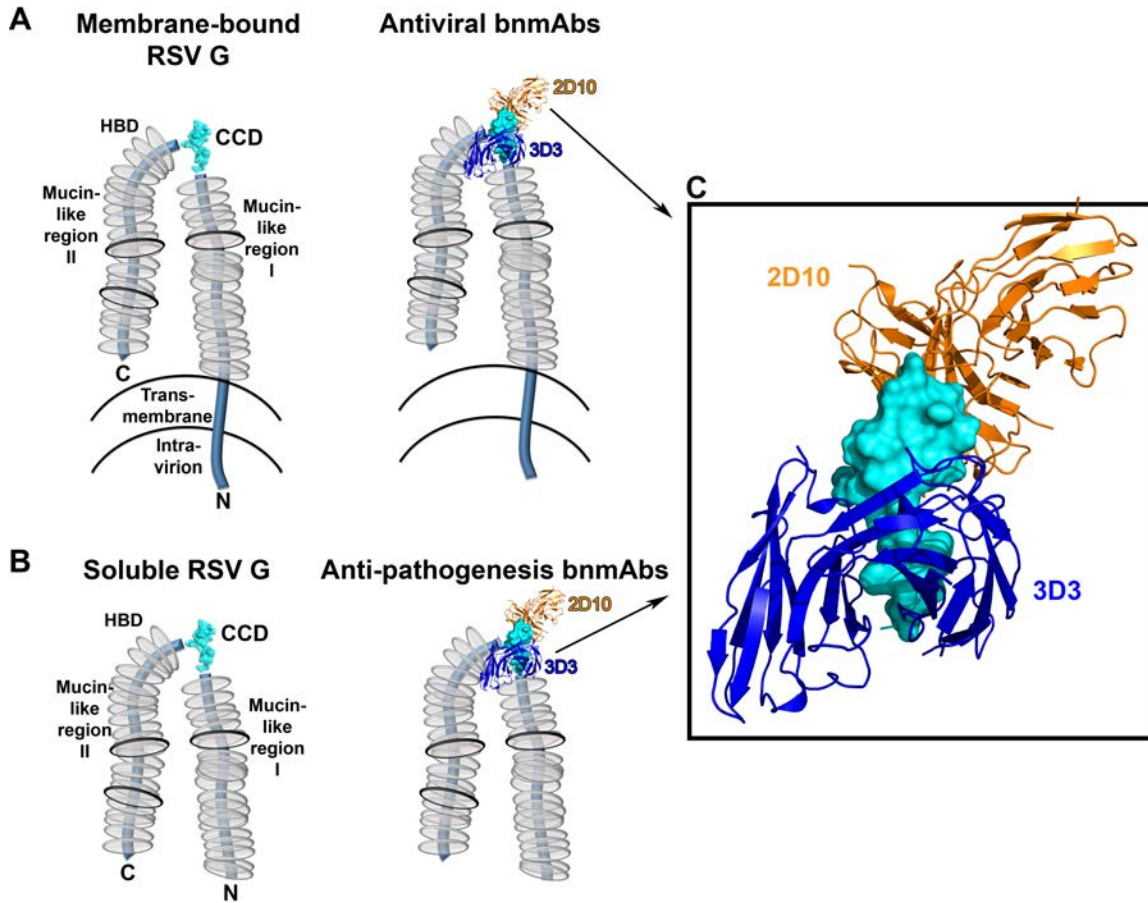


Fig. S3. Schematic of RSV G interactions with anti-G antibodies. (A) Model of membrane-bound G glycoprotein on the surface of the RSV virion or the surface of RSV-infected cells alone (left) or bound by bnmAbs 3D3 and 2D10 (right). (B) Model of soluble RSV G glycoprotein, which is secreted from RSV-infected cells and modulates CX3CR1⁺ immune cells, alone (left) or bound by bnmAbs 3D3 and 2D10 (right). (C) Zoom-in of RSV G CCD bound by bnmAbs 3D3 and 2D10. For clarity, only the variable regions of the bnmAbs are shown.

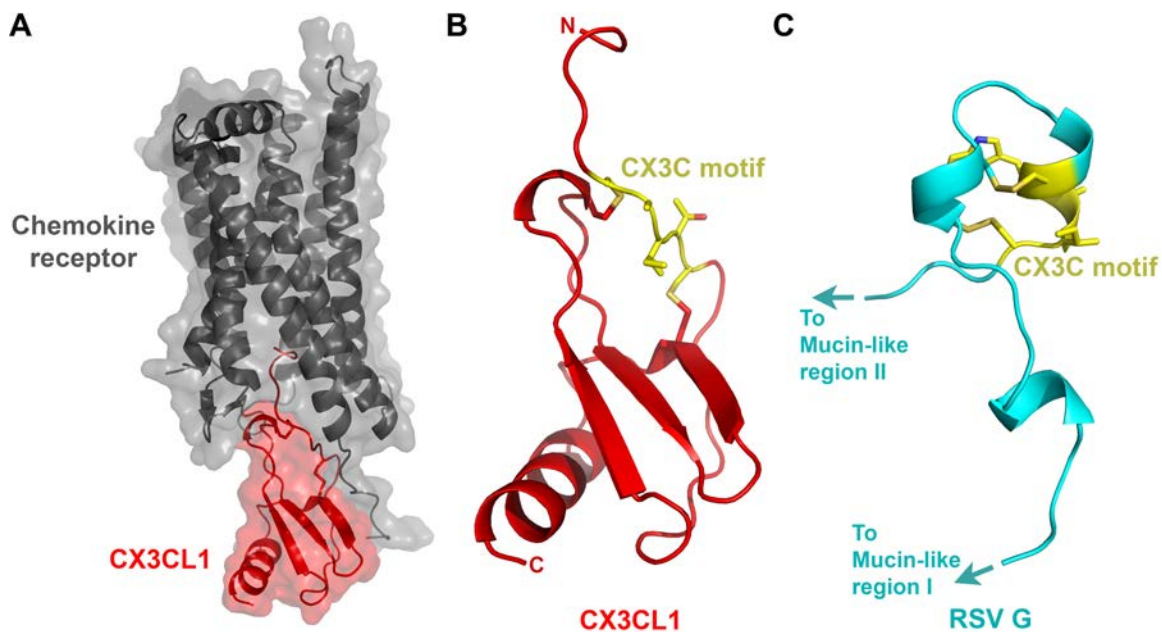
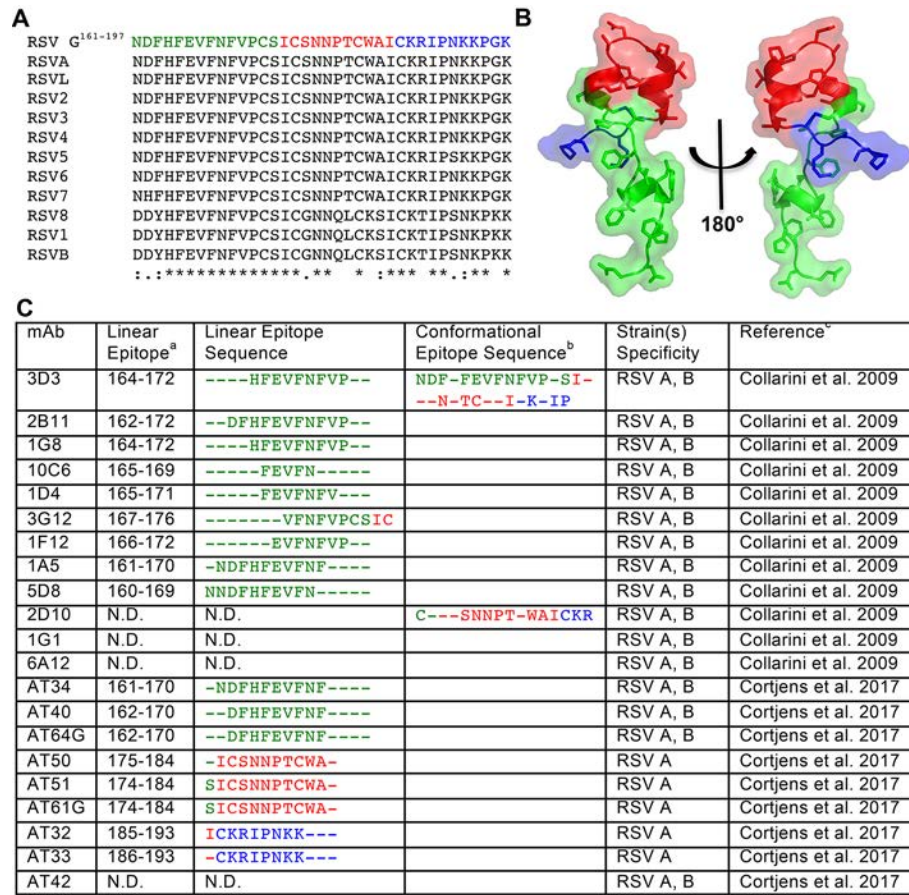


Fig. S4. Structural comparison of RSV G with CX3CL1 (fractalkine). (A) Structure of CX3CL1 (red) bound to the human cytomegalovirus G-protein coupled receptor US28 (grey) (PDB code 4XT1). US28 has 38% sequence identity with the human chemokine receptor CX3CR1. (B) Structure of CX3CL1 (red), in the same orientation as in panel a, with the amino acid side chains of the CX3C motif shown as sticks and colored yellow. (C) Structure of RSV G¹⁶¹⁻¹⁹⁷ (cyan), with the amino acid side chains of the CX3C motif shown as sticks and colored yellow. Images in panels B and C are shown at the same magnification.



^a Linear epitope sequence numbering in RSV strain A2. N.D. refers to no detectable binding to linear RSV

G peptides.

^b Conformational epitope sequences were determined in this study.

^c References for linear epitope sequence mapping.

Fig. S5. Isolated human anti-G mAbs and epitope characterization. (A) Sequence alignment of RSV G CCD from diverse RSV strains, colored by linear epitope clustering in three regions. **(B)** Structure of RSV G¹⁶¹⁻¹⁹⁷, colored as in panel a, revealing the overlap of linear epitopes in three-dimensional space. **(C)** Table of 21 isolated human anti-G mAbs, their linear epitope sequences, and their RSV strain specificity.

79 **Table S1. Crystallographic data collection and refinement statistics^a**

	3D3-RSV G¹⁶²⁻¹⁷²	3D3-RSV G¹⁶¹⁻¹⁹⁷	2D10-RSV G¹⁶⁹⁻¹⁹⁸
PDB code	5WNB	5WNA	5WN9
Data collection^b			
Space group	<i>P</i> 2 ₁ 2 ₁ 2 ₁	<i>P</i> 2 ₁	<i>P</i> 2 ₁ 2 ₁ 2 ₁
Cell dimensions			
<i>a</i> , <i>b</i> , <i>c</i> (Å)	68.76, 105.43, 121.82	64.62, 135.01, 73.78	44.84, 56.39, 126.15
α, β, γ (°)	90, 90, 90	90, 107.45, 90	90, 90, 90
Resolution (Å)	48.38 - 2.40 (2.48 - 2.40)	48.72 - 2.40 (2.48 - 2.40)	50.00 - 1.55 (1.58 - 1.55)
Total no. reflections	368,399	294,679	453,130
No. unique reflections	40,103	46,906	47,198
<i>R</i> _{merge} ^c	0.122 (0.838)	0.107 (0.763)	0.058 (0.930)
<i>I</i> / σ(<i>I</i>)	13.4 (3.1)	12.3 (2.2)	44.0 (1.4)
Completeness (%)	99.9 (99.8)	99.5 (99.0)	99.9 (99.4)
Redundancy	9.2 (8.3)	6.3 (5.6)	9.6 (6.2)
CC _{1/2} ^d	0.997 (0.808)	0.996 (0.670)	0.998 (0.751)
Refinement			
Resolution (Å)	48.38 - 2.40	48.72 - 2.40	50.00 - 1.55
No. reflections	35,325	46,869	47,114
<i>R</i> _{work} / <i>R</i> _{free} ^e	0.224 / 0.267	0.192 / 0.246	0.169 / 0.185
No. atoms			
Protein	6,552	7,124	3,810
Ligand/ion	22	None	None
Water	90	135	111
<i>B</i> -factors (Å ²)			
Protein: bnmAb	50	41	38
Protein: RSV G	40	56	48
Ligand/ion	63	None	None
Water	35	39	38
R.m.s. deviations			
Bond lengths (Å)	0.005	0.006	0.008
Bond angles (°)	0.864	0.935	0.968
Ramachandran (%)			
Favored	96.5	97.6	99.2
Allowed	3.5	2.4	0.8
Outliers	0	0	0

80 ^a For each structure, data from one crystal was used.81 ^b Values in parentheses are for highest-resolution shell.82 ^c *R*_{merge} = Σ(|*I* - <*I*>|) / Σ(*I*), where *I* is the observed intensity.83 ^d CC_{1/2} = Pearson correlation coefficient between random half-datasets.84 ^e *R*_{work} = Σ||*F*_o| - |*F*_c|| / Σ|*F*_o| for all data except 5%, which were used for *R*_{free} calculation.